
Competitive Removal of Cu^{2+} , Zn^{2+} and Ni^{2+} by Iron Oxide (Fe_3O_4) Nanomaterial

Shahlaa E. Ebrahim
Asst. Prof
Hasanain S. Alhares
College of Engineering
Baghdad University
Baghdad\ Iraq

Abstract:-

A competitive adsorption of Cu^{2+} , Ni^{2+} and Zn^{2+} ions from a synthetic wastewater onto (Fe_3O_4) nanomaterial was studied. Experimental parameters included pH, initial metal concentrations, and temperature was studied to obtain equilibrium data for adsorption, onto nanosorbent. The results indicate that the uptake capacities were 11.5, 6.07 and 9.68 mg/g for Cu^{2+} , Ni^{2+} and Zn^{2+} , respectively, onto nanosorbent. The best values of pH and contact time were 6 and 50 min., respectively. For these metals, the equilibrium isotherm for single component is of a favorable type and Freundlich model gave the best model for representing the experimental data. The Combination of Langmuir- Freundlich model best represented the isotherms binary and ternary component systems. In single, binary and ternary component systems, Cu^{2+} was always adsorbed more favorable onto nanosorbent than Zn^{2+} and Ni^{2+} . The results of thermodynamic study showed that the adsorption process is endothermic and physical nature.

1. Introduction

Presence of heavy metals in wastewaters causes significant environmental problems. High concentrations of heavy metals are known to be toxic and carcinogenic for living organisms. When heavy metals are present even in a very low concentration, their concentration may be elevated through bio-magnification

to a level that they start to exhibit toxic characteristics. Therefore, heavy metals are major pollutants in many industrial wastewaters and are toxic to human and aquatic life [49]. Due to their elemental non-degradable nature, heavy metals, regardless of their chemical form, pose serious ecological risk, when released into the environment. The metals which are of greatest environmental concern are

cadmium, mercury, lead, chromium, cobalt, copper, nickel and zinc [40]. The presence of heavy metal ions in the environment are detected in the waste streams from different industrial activities such as mining operations, tanneries, electronics, electroplating, petroleum refineries, and petrochemical industries [8].

The toxicity of heavy metals can be listed in order of decreasing toxicity as $Hg > Cd > Cu > Zn > Ni > Pb > Cr > Al > Co$, although this is only approximate as the vulnerability of species to individual metals varies. Toxicity also varies according to environmental conditions that control the chemical speciation of the metals [13; 41].

Heavy metals can pose health hazards if their concentration exceeds the allowable limits. As they are non-biodegradable, and persistence their threat is multiplied by their accumulation in the environment elements such as food chain and thus poses a significant danger to human health and life [28].

The removal of heavy metals ions from wastewater involves high cost techniques such as ion-exchange, evaporation, precipitation, membrane separation etc. However, these common techniques are too expensive to treat low levels of heavy metals in wastewater. Adsorption techniques are widely used in the field of removing small quantities of pollutant present in large volume of fluid, which can be

carried out in batch wise or continuous manner of operation [38]. Many factors that affect the decision of choosing an adsorbent for removal of pollutants from water are: economical factor (cost of the adsorbent), abundance, availability and effectiveness of the adsorbent [47].

The last decade has seen a continuous improvement in the development of effective/noble adsorbents in the form of activated carbon [21], zeolites [37], clay minerals [19], chitosan [4], lignocelluloses [44], natural inorganic minerals [42], functionalized polymers [36], etc. However, most of these adsorbents are either not effective (due to diffusion limitation or the lack of enough active surface sites) or have shown problems like high cost, difficulties of separation from wastewater, or generation of secondary wastes. Nowadays there is a continuously increasing worldwide concern for the development of using nano-adsorbents viz. nano-alumina [46], functionalized carbon nanotubes [16], and hydroxyapatite nanoparticles [12], which have demonstrated high adsorption efficiency for metal ions removal. The utilization of iron oxide nanomaterials has received much attention due to their unique properties, such as extremely small size, high surface-area-to-volume ratio, surface modifiability, excellent magnetic properties [53]. One such advanced class of adsorbent – magnetic nano-

adsorbent with the help of an external magnetic field has been further successful in circumventing the solid–liquid separation problem usually encountered with nanoparticle. Such adsorbent combining nanotechnology and magnetic separation technique has not only demonstrated high adsorption efficiency due to its large surface to volume ratio, but have also shown additional benefits like ease of synthesis, easy recovery and manipulation via subsequent coating and functionalization, absence of secondary pollutants, cost-effectiveness and environmental friendliness [15]. Several magnetic nanomaterials, including maghaemite nanoparticles [20], Fe_3O_4 magnetic nanoparticles [43], Fe_3O_4 nanoparticles functionalized and stabilized with compounds like humic acid [27] have been explored for the removal of metal ions. In nanotechnology focuses on the fabrication of nano-sized adsorbents with enhanced adsorption capacity and rapid sorption rate for the removal of target contaminants. This is due to the large surface area and highly active surface sites of the nanoadsorbents [6].

Iron oxide nanoadsorbents are cost-effective adsorbents that provide high adsorption capacity, rapid adsorption rate and simple separation and regeneration [32]. The present study is to evaluate the competitive adsorption of heavy metals (Zn, Cu and Ni) as

inorganic pollutants from wastewater by nanosorbent (Fe_3O_4), for removal of heavy metals in batch reactors at different operating condition in single, binary and ternary systems.

2. Equilibrium Isotherm Batch Models for Nano sorbent

2.1 Single Component System

Empirical models are simple mathematical relationships, characterized by a limited number of adjustable parameters, which give a good description of the experimental behavior over a large range of operating conditions. The model used to describe the results should be capable of predicting sorbate binding at both low and high concentrations [51].

Although these conventional empirical models do not reflect the mechanisms of sorbate uptake, they are capable of reflecting the experimental curves of adsorption isotherm [51].

2.1.1 Langmuir Model (1916)

The Langmuir model can be represented as:

$$q_e = \frac{q_{max}bC_e}{(1+bC_e)} \quad (1)$$

Where q_e is the amount of adsorbate adsorbed per mass of adsorbent (mg/g). C_e is the equilibrium concentration (mg/l).

This classical model incorporates two easily interpretable constants: q_{\max} , which corresponds to the maximum achievable uptake by a system; and b , which is related to the affinity between the sorbate and sorbent, (l/mg). The Langmuir constant “ q_{\max} ” is often used to compare the performance of biosorbents; while the other constant “ b ” characterizes the initial slope of the isotherm. Thus, for a good biosorbent, a high q_{\max} and a steep initial isotherm slope (i.e., high b) are generally desirable. [1; 24] the Langmuir model assumes the following: (i) the surface consists of adsorption sites, (ii) all adsorbed species interact only with a site and not with each other, (iii) adsorption is limited to a monolayer, and (iv) adsorption energy of all the sites is identical and independent of the presence of adsorbed species on neighboring sites. [39]

Each component is adsorbed onto the surface according to ideal solute behavior; there is no interaction or competition between molecules involved under homogenous conditions [30].

The important characteristic of the Langmuir isotherm can be expressed in terms of dimensionless constant separation factor for equilibrium parameter R_L . This is defined by [40]:

$$R_L = \frac{1}{b + C_0} \quad (2)$$

[7] Show, using mathematical calculation, that the parameter R_L indicates the shape of isotherm as follows in Table. 1.

Table.1 Constant parameter R_L

R_L	Type of isotherm
$R_L > 1$	unfavorable
$R_L = 1$	linear
$R_L = 0$	irreversible
$0 < R_L < 1$	favorable

2.1.2 Freundlich Model (1918)

The Freundlich isotherm can be represented as:

$$q = KC_e^{1/n} \quad n > 1 \quad (3)$$

The Freundlich isotherm was originally empirical in nature, but was later interpreted as the sorption to heterogeneous surfaces or surfaces supporting sites with various affinities. It is assumed that (i) the stronger binding sites are initially occupied, (ii) the binding strength decreasing with increasing degree of site occupation. It incorporates two constants: K , which corresponds to the maximum binding capacity; and n , which characterize the affinity between the sorbent and sorbate (adsorption intensity). [51]

2.1.3 Redlich–Peterson Model (1959)

$$q_e = \frac{K_{RP}C_e}{1 + a_{RP}C_e^{\beta_{RP}}} \quad (4)$$

Redlich–Peterson isotherm shows that an “area of stability” is reached after a frequent rise in the curve, i.e., several layers of adsorption occurs first. This isotherm assume (i) equilibrium for heterogeneous surfaces as it contains the heterogeneity factor β . (ii) It also converges to Henry’s law at low surface coverage and is, therefore, (iii) thermodynamically consistent. However, it does not have as wide a practical application as the Langmuir and the Freundlich isotherms due to the inconvenience of evaluating three isotherm constants [25].

β_{RP} has values between 0 and 1. For $\beta_{RP} = 1$ the Redlich–Peterson model converts to the Langmuir model. $\beta_{RP}=0$ the Henry’s Law form results.

2.1.4 Sips Model (1948)

$$q_e = \frac{K_s C_e^{\beta_s}}{1 + a_s C_e^{\beta_s}} \quad (5)$$

K_s is the Sips model isotherm constant; a_s the Sips model constant; β_s the Sips model exponent. This equation is also called Langmuir–Freundlich isotherm and the name derives from the limiting behavior of the equation. At low sorbate concentrations it effectively reduces to a Freundlich isotherm and thus does not obey Henry’s law. At high sorbate concentrations, it predicts the monolayer sorption capacity characteristics of the Langmuir isotherm [39].

2.1.5 Khan Model (1997)

$$q_e = \frac{q_{max} b_k C_e}{(1 + b_k C_e)^{a_k}} \quad (6)$$

b_k is the Khan model constant; a_k Khan model exponent, q_{max} maximum uptake [51].

2.1.6 Toth Model (1971)

$$q_e = \frac{q_{max} b_T C_e}{\left[1 + (b_T C_e)^{\frac{1}{n_T}}\right]^{n_T}} \quad (7)$$

b_T the Toth model constant and n_T the Toth model exponent [51].

It derives from potential theory and is used in heterogeneous systems. Toth model assumes a quasi-Gaussian energy distribution; most sites have adsorption energy lower than the peak of maximum adsorption energy [22].

2.2 Multi Component Systems

The adsorption of the solute of interest not only depends on the adsorbent surface properties and physical–chemical parameters of a solution such as pH and temperature, but also on the number of solutes and their concentrations. In such cases, the adsorption will become competitive, with one solute competing with another to occupy the binding sites [52].

Multicomponent biosorption has been the subject of limited studies. The uptake of a given metal ion is

decreased to a greater extent in ternary combinations and furthermore in quaternary systems compared to the binary combinations. In the presence of co-ions in solution, chemical interactions between the ions themselves as well as with the adsorbent take place resulting in site competition. Therefore metal uptake from multicomponent systems is lower.

For binary solute cases, different isotherm models have been used to correlate single-solute isotherm data and to describe multi-solute sorption isotherms based on the time-consuming iterative algorithm [7].

2.2.1 Extended Langmuir Model (ELM)

$$q_i = \frac{b_i q_{m,i} C_{e,i}}{1 + \sum_{j=1}^n b_j C_{e,j}} \quad (8)$$

Where $C_{e,i}$ is the equilibrium concentration of the component i in the multicomponent solution, q_i is the equilibrium uptake of the component i , b_i and $q_{m,i}$ are the Langmuir isotherm model parameters obtained suitably from Eq. (1) in the single solute system. This model assumes (i) homogeneous surface with respect to the energy of sorption, (ii) no

interaction between adsorbed species and (iii) that all sorption sites are equally available to all adsorbed species [1].

2.2.2 Redlich-Peterson Model

The three-parameter isotherm of Redlich-Peterson that has been empirically developed for multi-component mixtures is given as [11; 48]:

$$q_i = \frac{K_{R,i} q_{m,i} C_{e,i}}{1 + \sum_{j=1}^n a_{R,j} C_{e,j}^{B_j}} \quad (9)$$

Where $K_{R,i}$ and $q_{m,i}$ are the Redlich-Peterson isotherm-model parameter suitably obtained from equation(4) in single solute system.

2.2.3 Combination of Langmuir-Freundlich Model

The competitive model related to individual isotherms parameters are expressed in the following equation [45]:

$$q_i = \frac{q_{m,i} b_i C_{e,i}^{\left(\frac{1}{n_i}\right)}}{1 + \sum_{j=1}^n b_j C_{e,j}^{\left(\frac{1}{n_j}\right)}} \quad (10)$$

A stock solution of copper, nickel and zinc ions with a concentration of (1000 mg/l) were prepared by using $\text{Cu}(\text{NO}_3)_2$, $\text{Ni}(\text{NO}_3)_2$ and $\text{Zn}(\text{NO}_3)_2$ (minimum purity 99.5%). Weights of

3.805, 4.945 and 4.548g of copper nitrate, nickel nitrate and zinc nitrate, respectively were dissolved in 200 ml of distilled water.

A volume of 10 ml concentrated HNO_3 was added then it was diluted to 1000 ml with distilled water [3]. Concentrations of 50 mg/l from these salts were used as adsorbate for different weights of nanosorbent. All the glassware used for dilution, storage and experiments were cleaned with

extra detergent, thoroughly rinsed with tap water, soaked overnight in a 20% HNO_3 solution and finally rinsed with distilled water before use. Dissolved metal concentrations in solution were determined by a flame atomic absorption spectrophotometer (Buck, Accusys 211, USA).

Table. 2 shows the main physicochemical properties of the metals tested

Table.2 Main physicochemical properties of the metals tested

Properties	Copper	Nickel	Zinc
Formula	Cu^{2+} from $\text{Cu}(\text{NO}_3)_2$	Ni^{2+} from $\text{Ni}(\text{NO}_3)_2$	Zn^{2+} from $\text{Zn}(\text{NO}_3)_2$
Appearance	blue crystals	Emerald green solid	colorless crystals
Molar mass ($\text{g}\cdot\text{mol}^{-1}$)	241.6	290.79	297.49
Standard atomic weight	63.546	58.6934	65.38
Atomic Radius(pm)	128	124	134
Van der Waals radius(pm)*	140	163	139
Electronegativity (Pauling scale)**	1.9	1.91	1.65
Company	BDH (England)	Fluka (Switzerland)	SCHARLAU (Spain)

* pico meter = 10^{-12} m.

**Pauling Scale: A dimensionless quantity, on a relative scale running from around 0.7 to 3.98 (Hydrogen was chosen as the reference, its electronegativity was fixed first at 2.1, later revised to 2.20).

3.2 Nanosorbent

(Fe_3O_4) nanoparticles obtained from US Research Nanomaterials, Inc., Houston, TX 77084, (USA) were used as nanosorbents. The main physical

properties of the Nanopowder / Nanoparticules, Iron Oxide (Fe_3O_4) are listed in Table (3). Table (4) shows Certificate of Analysis --% of Iron oxide Nanoparticules (Fe_3O_4).

Table.3 The main physical properties of the Nanosorbent

Physical Properties of the Nanosorbent, Iron Oxide (Fe ₃ O ₄)	
Purity	98+%
Average Particle Size	20-30 nm
Surface Area	40-60 m ² /g
Color Dark	Dark Brown
Morphology	spherical
Bulk Density	0.84 g/cm ³
True Density	4.8-5.1 g/cm ³

Table.4 Certificate of Analysis --% Iron oxide Nanoparticales

Certificate of Analysis --% Iron oxide Nanoparticales (Fe ₃ O ₄)				
Ca	Cr	K	Mn	SiO ₂
0.02290<	0.0016<	0.0012<	0.086<	0.142<

The characteristics of the selected nanosorbents were evaluated; namely: specific surface area, and external surface area. Results are presented in Table. 5. External and specific surface areas of the nanosorbent were measured in Ministry of Oil /

Petroleum Development and Research Centre. The results show that there is no significant difference between them. This indicates that the nanosorbents have no significant porosity and maintain a high external surface area.

Table. 5 Characterizations of Fe₃O₄ nanosorbents considered in this study.

Manufacturer reported surface area (m ² /g)	Specific surface area (m ² /g)	External surface areas(m ² /g)
40-60	63	61

3.2.1 Adsorption Experiments

A series of experiments were carried out in a batch system to obtain equilibrium data for adsorption of single, binary and ternary metals solutions.

Table.6 shows the major varied parameters used in these experiments.

Table.6 Major experimental parameters that varied in batch experiments

	Parameter	Range	Purpose
Batch	pH	3, 4, 5 ,6 and 7	To find the best pH of removal efficiency.
	Nanosorbent weight	0.05, 0.1, 0.2, 0.4, 0.6,0.8, 1,1.2, and 1.4 g	To plot the equilibrium isotherm curves.
	Temperature	20, 35, and 50 °C	To study the thermodynamic parameters of adsorption.
	Initial conc.	10, 50, 100, and 150 ppm	To study the effect of initial conc. on the adsorption.

3.2.2 Batch Experiments for Nanosorbent

3.2.2.1 Determination of the best pH

The effect of pH on Cu^{2+} , Zn^{2+} and Ni^{2+} ions adsorption onto nanosorbent was studied; 0.5 g nanosorbent of Fe_3O_4 was mixed with 100 ml of single metal ion solutions with concentration of 50 mg/l of Cu^{2+} , Zn^{2+} and Ni^{2+} ions respectively. To maintain at different pH values (ranging from 3 to 7) 0.1 M NaOH or HNO_3 were added. The solutions were agitated at 200 rpm for a period of 30 min and at room temperature. Separation of nanosorbents from the aqueous solution was evaluated by a small horseshoe magnet and wearing specific suits, thick gloves, special eye glasses, and special mask to prevent the direct contact with nanomaterial. Samples (10 ml) were taken from each volumetric flask and measured by using AAS.

3.2.2.2 Equilibrium Isotherm Experiments

Different weights of Fe_3O_4 nanosorbent were used, (0.05, 0.1, 0.2, 0.4, 0.6, 0.8, 1, 1.2, and 1.4 g). A sample of 100 ml of measured concentration solution of 50 mg/l was used for single, binary and ternary system systems of Cu^{2+} , Zn^{2+} and Ni^{2+} respectively. The pH of the metal solutions was adjusted to the optimum pH value. The samples were then placed on a shaker (HV-2 ORBTAL, Germany) and agitated continuously for 50 min at 200 rpm and. A few drops of 0.1M HNO_3 were added to samples after separation of nanosorbent from aqueous solution to decrease the pH value below 2 in order to fix the concentration of the heavy metals during storage before analysis [3]. The final equilibrium concentrations were measured by AAS . The adsorbed amount is then calculated by the following equation:

$$q_e = \frac{V_1(C_o - C_e)}{W_{(\text{nanosorbent})}} \quad (11)$$

The adsorption isotherms were obtained by plotting the weight of solute adsorbed per unit weight of

biomass (q_e) against the equilibrium concentration of the solute in the solution (C_e) [51].

3.2.2.3 Thermodynamic Parameters of Adsorption

The effect of temperature on Cu^{2+} , Zn^{2+} and Ni^{2+} ions adsorption uptake onto nanosorbent was studied, 0.6 g of nanosorbent was mixed with 100 ml of single metal ion solutions with concentration of 50 mg/l of Cu^{2+} , Zn^{2+} and Ni^{2+} respectively. They were maintained at different temperature values ranged from 20 to 50°C for a contact time of 50 min and agitation speed was 200 rpm. Samples (10 ml) were taken from each volumetric flask and measured by AAS.

4. Results and Discussion

4.1 Effect of pH

Fig.. 1 shows the effect of different pH values on the adsorption uptake of Cu^{2+} , Zn^{2+} and Ni^{2+} ions onto Fe_3O_4 nanosorbent. Beyond pH 6.0 precipitations of insoluble metal hydroxides will start and make the true sorption studies impossible. At low pH, proton would compete for active binding sites with metal ions. The protonation of active sites tends to decrease the metal sorption. At low pH around 2 all the binding sites may be protonated, thereby desorbing all originally bound metals from the biomass [2]. Therefore, optimum

copper, zinc and nickel ions adsorption process will be at pH 6. These results agreed with the results obtained by [32], and [14].

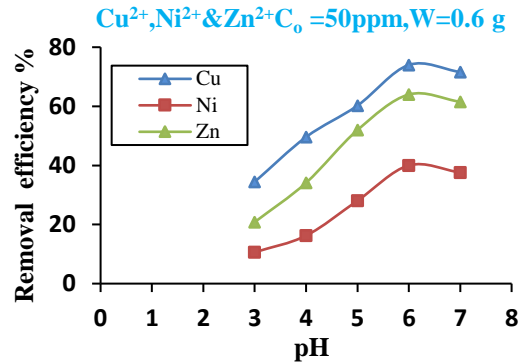


Fig. 1 Effect of different pH values on copper, zinc, nickel ions uptake by NMOs, $C_{\text{nanosorbents}} = 6\text{g/l}$, $C_0(\text{Cu, Zn and Ni}) = 50\text{mg/l}$.

4.2 Effect of Contact Time

For all batch experiments, the contact time should be fixed at a value to ensure reaching equilibrium concentrations. A weight of 0.6 g of nanosorbent (Fe_3O_4) was mixed with 100 ml of single metal ion solutions concentration of 50 mg/l of Cu^{2+} , Zn^{2+} and Ni^{2+} ions at pH 6. These were maintained at different time values ranging from 10 to 70 min. Fig.. 2 shows the results of removal efficiency (%) with the contact time of the metal solutions. It can be concluded that 50 min contact time is sufficient to reach equilibrium condition for each metal.

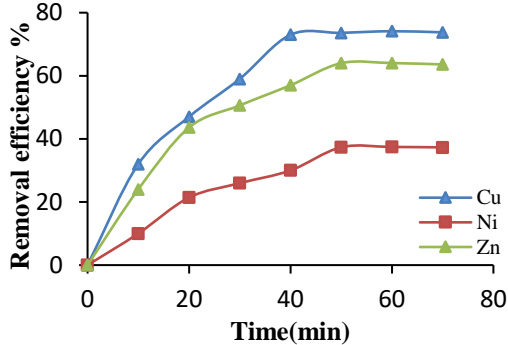


Fig. 2 Adsorption efficiency for nanosorbent with different contact times, $C_0=50$ mg/l, pH=6, w=0.6 g, 200 rpm

4.3 Effect of Initial Heavy Metal Concentration

Different concentrations of 10, 50, 100 and 150 mg/l were selected to study the variation of removal efficiency with different initial concentrations at the same weight of nanosorbent (1g) and at room temperature. The pH of heavy metal solutions was fixed at the optimum value 6, and the agitation speed of the shaker was 200 rpm for contact time of 50min. as shown in Fig.. 3.

It can be seen that the percentage removal efficiency was not altered greatly if the concentration increased from 10 to 50 mg/l. This behavior due to that 1 g of nanosorbent may contain enough sites .when the concentrations increase to 100 and 150 mg/l the sites in 1 g will not be enough to accumulate these concentrations so that the depletion in percentage removal efficiency was obvious.

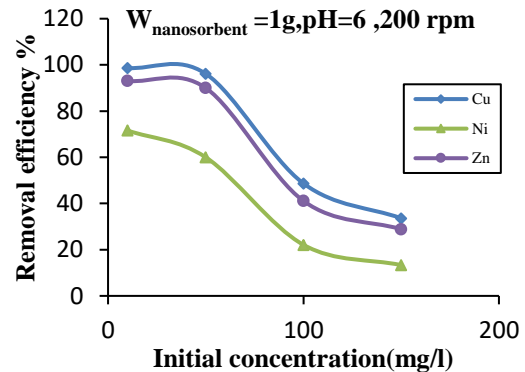


Fig. 3 Percentage of removal adsorption efficiency with variation of initial concentration, contact time 50 min and 200rpm

4.4 Effect of Temperature and Thermodynamic Parameters

The effect of temperature on the equilibrium sorption capacity for Cu^{+2} , Ni^{+2} , and Zn^{+2} ions had been investigated at a temperature range between 20-50 °C. Fig.4 shows the variation of percentage removal efficiency with temperature. It can be concluded that the increase in temperature leads to increase the percentage removal efficiency. The variation of temperature from 20-30 °C has a small significant effect on the adsorption process, so that the adsorption experiments can be carried out at room temperature without any adjustment.

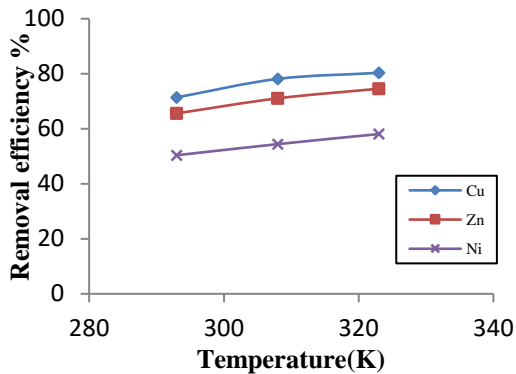


Fig. 4 Variation of percentage removal with solution temperature, $C_0=50$ mg/l, contact time 50min, $W_{\text{nanosorbent}}=0.6$ g, and 200rpm

Thermodynamic parameters were obtained by varying the temperature over the range 20 to 50°C by keeping other variables constant. The values of the thermodynamic parameters such as ΔG° , ΔH° and ΔS° , describing copper, zinc and nickel ions uptake by nanosorbent, were calculated using the thermodynamic equations:

$$\Delta G = -RT \ln(K_c) \quad (12)$$

Where

$$K_c = \frac{C_{\text{ad}}}{C_e} \quad (13)$$

Where K_c is the equilibrium constant, C_{ad} is the amount of metal adsorbed on the biosorbent per liter of the solution at equilibrium (mg/l), C_e is the equilibrium concentration of the metal in the solution (mg/l), T is absolute temperature (K) and R is the universal gas constant (8.314 J/mol K). Also, enthalpy changes (ΔH) and entropy

changes (ΔS) can be estimated by the following equation [10].

$$\Delta G = \Delta H - \Delta ST \quad (14)$$

The thermodynamic parameters, Gibbs free energy change ΔG° , standard enthalpy change ΔH° , and standard entropy change ΔS° are used to understand the effect of temperature on the biosorption process [17].

Table. 7 Thermodynamic constants of adsorption obtained for Cu^{+2} , Zn^{+2} and Ni^{+2} ions sorption onto nanoadsorbent.

Met al	Temperatu re (K)	ΔG° (kj.mol ⁻¹)	ΔH° (kj.mol ⁻¹)	ΔS° (j.mol ⁻¹ K ⁻¹)	R ²
Cu ⁺²	293	-2.2305	12.8	0.051	0.964
	308	-3.2605			
	323	-3.7792			
Zn ⁺²	293	-1.5713	11.25	0.043	0.996
	308	-2.2994			
	323	-2.8871			
Ni ⁺²	293	-0.0359	7.119	0.024	0.999
	308	-0.41427			
	323	-0.7686			

Generally, the change in adsorption enthalpy for physisorption is in the range of -20 to 40 kJ mol⁻¹, but chemisorptions is between -400 and -80 kJ mol⁻¹ [54].

Fig.. 5 and Table. 7 show the thermodynamic constants of adsorption

obtained for Cu^{2+} , Zn^{2+} and Ni^{2+} ions onto nanosorbents.

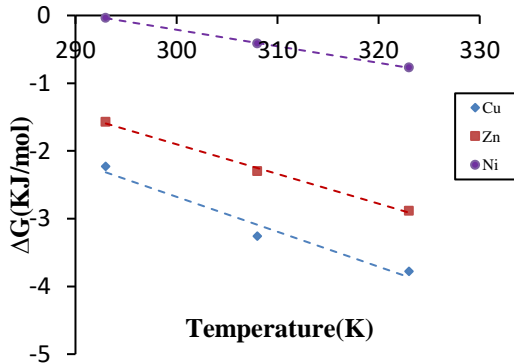


Fig.5 Change in free energy with temperature for the adsorption of Cu^{2+} , Zn^{2+} and Ni^{2+} ions by nanosorbent at initial concentration of 50 mg/l, and pH 6.

Table.7 shows the values of enthalpy ΔH° were 12.8, 11.25 and 7.119 $\text{kJ}\cdot\text{mol}^{-1}$ for Cu^{2+} , Zn^{2+} and Ni^{2+} ions respectively, reveal that the adsorption is endothermic and physical in nature. This is also supported by the increase in the values of uptake capacity of nanosorbents with the rise in temperature. The positive values of entropy ΔS° were 0.051, 0.043, 0.024 $\text{J}\cdot\text{mol}^{-1}\text{K}^{-1}$, reflect the affinity of Cu^{2+} , Zn^{2+} and Ni^{2+} ions to be adsorbed onto nanosorbent [34]. The decrease in the value of the free energy ΔG° with the

increase in temperature indicates that the adsorption process is endothermic and it is thereby favored with the increase in temperature, thus, the process is better carried out at high temperature [17].

4.5 Estimation of Adsorption Isotherms Constants

The adsorption for a single, binary and ternary component systems of Cu^{2+} , Zn^{2+} and Ni^{2+} ions onto Fe_3O_4 in batch experiments were conducted with initial concentration of (50 mg/l) and particle size of (20-30 nm) at room temperature in order to determine the isotherm constants for each system using different isotherm models.

4.6 Single Component System

The adsorption isotherm for single component systems of Cu^{2+} , Zn^{2+} and Ni^{2+} ions respectively, onto nanosorbent are shown in Figs. 6 to 8, whereas Fig.. 9 shows a comparison between them. The data, for single component systems were correlated with six models illustrated in section (2.1).

The parameters for each model obtained from non-linear statistical fit of the equation to the experimental data (STATISTICA software, version 6). Table. 8 shows parameters of single solute isotherm for Cu^{2+} , Zn^{2+} and Ni^{2+} ions uptake onto nanosorbent.

Figs. 10 to 12 show comparison of some selective models applied in single system for copper, zinc and nickel ions respectively.

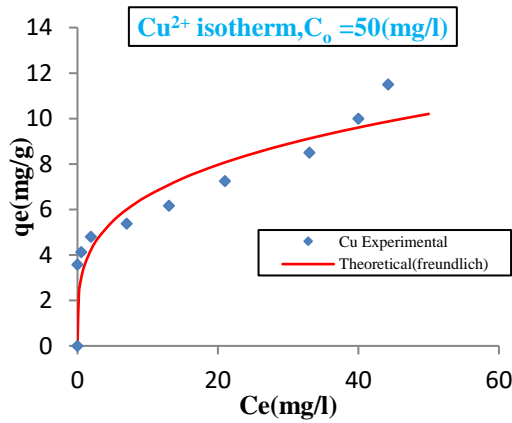


Fig.6 Adsorption isotherm for copper ions onto nanosorbent

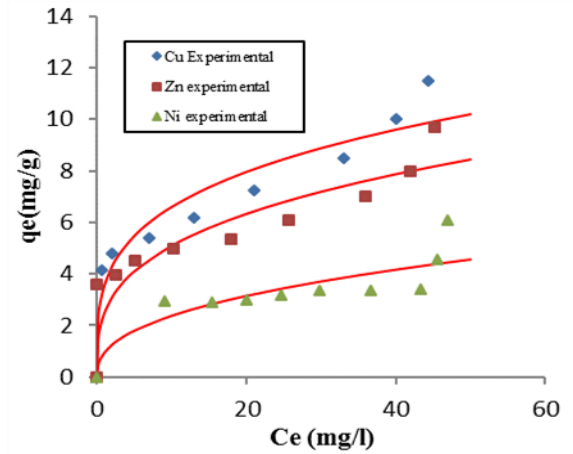


Fig.9 Adsorption isotherms of Cu, Zn and Ni ions as single solutes onto nanosorbent

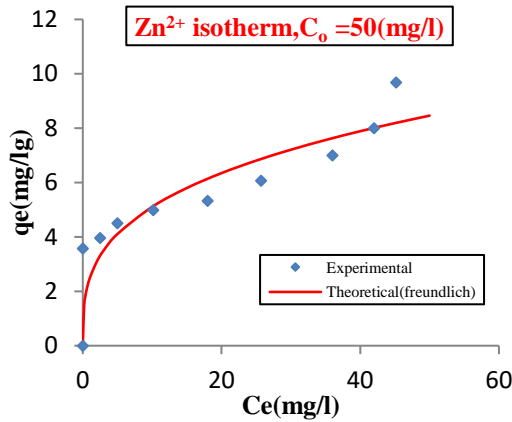


Fig.7 Adsorption isotherm for zinc ions onto nanosorbent

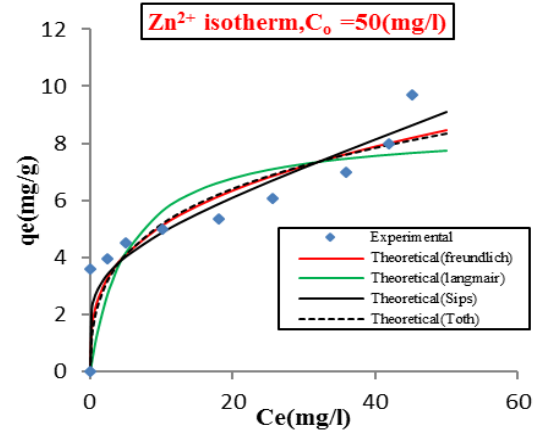


Fig.10 Comparison of some selective models applied in single system for zinc ions onto nanosorbent

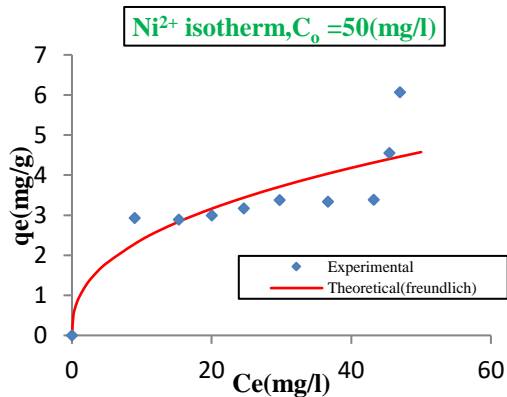


Fig.8 Adsorption isotherm for nickel ions onto nanosorbent

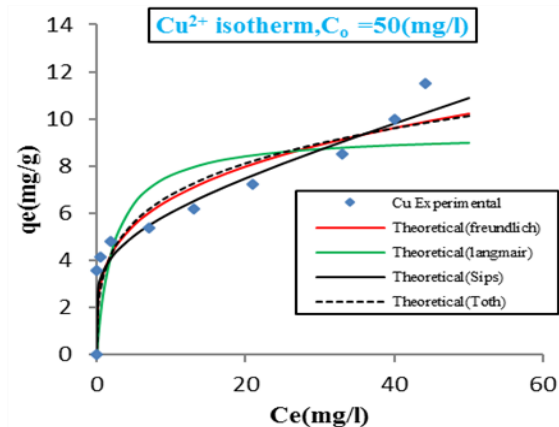


Fig.11 Comparison of some selective models applied in single system for copper ions onto nanosorbent

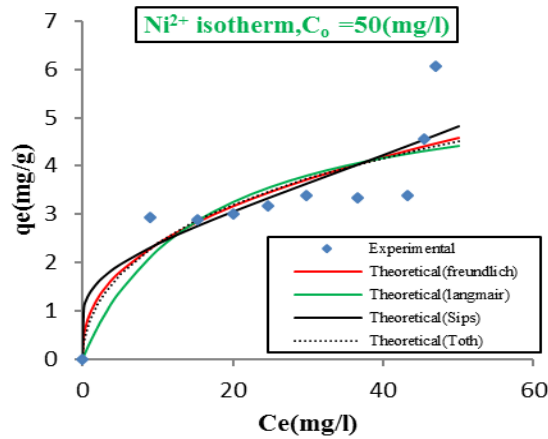


Fig.12 Comparison of some selective models applied in single system for nickel ions onto nanosorbent

Table. 8 Parameters of single solute isotherm for Cu²⁺, Zn²⁺ and Ni²⁺ ions for nanosorbent

MODEL	PERAMETER	SINGLE		
		Cu ⁺²	Zn ⁺²	Ni ⁺²
Langmuir $q = \frac{bq_m C_e}{1 + bC_e}$ [26]	q _m (mg/g)	9.4223	8.5623	5.7933
	b(l/mg)	0.4247	0.19	0.0639
	R ²	0.8143	0.81	0.86
Freundlich $q = KC_e^{1/n}$ [33]	K, (mg/g)(mg/l) ^(1/n)	3.544	2.479	0.9446
	n,-	3.6695	3.1877	2.4801
	R ²	0.899	0.8537	0.8816
Table 8. continued				
Redlich–Peterson $q_e = \frac{K_{RP}C_e}{1 + a_{RP}C_e^{\beta_{RP}}}$ [31]	k _{RP} (mg/g)	0.2138	0.1625	1.562e13
	a _{RP} (l/mg)	-0.2283	-0.2571	1.913e13
	β _{RP} -	0.00002	.000026	0.556
	R ²	0.5604	0.495	0.8807
Sips $q_e = \frac{K_s C_e^{\beta_s}}{1 + a_s C_e^{\beta_s}}$ [45]	k _s , (l/g)	0.46034	0.40273	0.05114
	β	0.02268	0.0258	0.00684
	a _s , (l/mg)	-0.8729	-0.859	-0.963
	R ²	0.877	0.848	0.865
Khan $q_e = \frac{q_{max} b_k C_e}{(1 + b_k C_e)^{a_k}}$ [23]	q _m (mg/g)	0.6502	0.5597	0.34003
	b _k ,(l/mg)	513.204	113.107	12.7709
	a _k	0.728	0.686	0.59743
	R ²	0.8887	0.8436	0.8714

$q_e = \frac{q_{max} b_T C_e}{\left[1 + (b_T C_e)^{n_T}\right]^{1/n_T}}$ [51]	q_m (mg/g)	102.994	81.7608	44.5025
	b_T	736.78	20.39	0.4606
	n_T	8.789	7.1183	5.2311
	R^2	0.8908	0.8485	0.877

Figs. 6 to 12 and Table. 8 show the following:

- The equilibrium isotherm for each single component is of favorable type. $n > 1$.
- The adsorption capacity q_e and heavy metals removal rate were related to the amount of adsorbent added; the greater adsorption capacity was obtained at lower adsorbent dose, where the higher removal rate was achieved at higher adsorbent dose.
- The Freundlich model gives the best fit for the experimental data for single component adsorption system for copper, zinc and nickel ions recognized by the highest values of (R^2), this model has been used successfully to describe equilibrium adsorption. Results can be compared for the adsorbates in terms of maximum bending capacity and (n) parameters: $Cu^{2+} > Zn^{2+} > Ni^{2+}$.
- Copper and zinc which are the highest affinity order for being adsorbed by the nanosorbent, have the lowest hydration Van der Waals

radius while nickel ions the least favorable by the nanosorbent, has the highest hydration Van der Waals radius, Table. 2. This coincides with the fact that less hydrated ions radius is preferably accumulated at the interface [18].

- Sharing of electrons is involved in covalent binding. The binding strength increases with increasing polarizability of the ions [29]. From Table. 2 the electronegativities for copper is higher than zinc, therefore, copper ions has higher strength of covalent binding than the lower affinity zinc ion. As the electronegativity of the atom increases, its ionic forms seem to be more easily sorbed by the adsorbent [9].

4.7 Binary Component System

The data, for binary component systems were correlated with three models as mentioned in section (2.2). The parameters for each model obtained from non-linear statistical fit of the equation to the experimental data. The adsorption isotherms for

binary component systems of Cu^{2+} , Zn^{2+} and Ni^{2+} ions onto nonabsorbent are shown in Figs 13 to 15.

Table. 9 represent all parameters with correlation coefficient for binary systems.

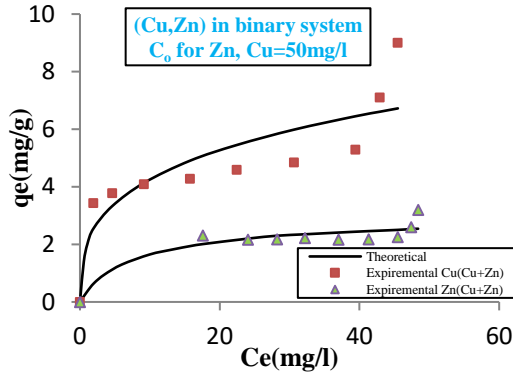


Fig.13 Adsorption isotherms of copper and zinc ions onto nanosorbent

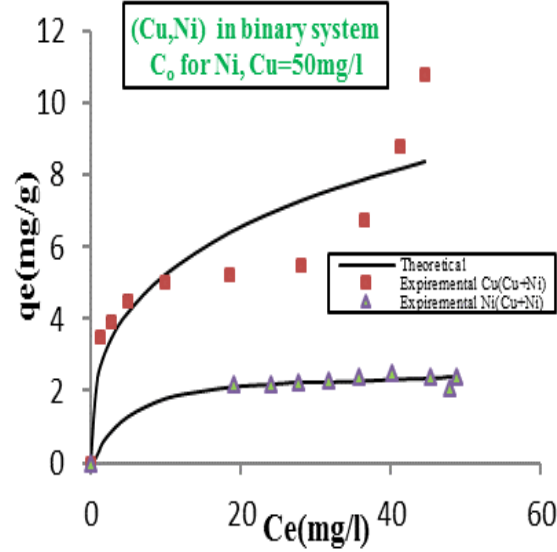


Fig.14 Adsorption isotherms of copper and nickel ions onto nanosorbent

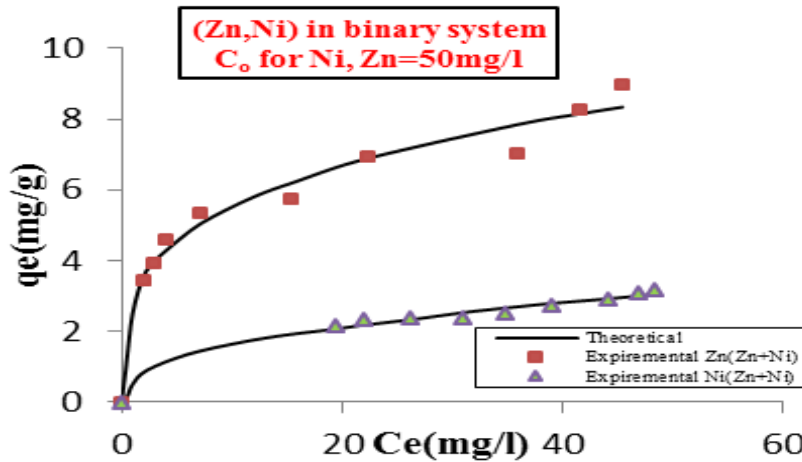


Fig.15 Adsorption isotherms of zinc and nickel ions onto nanosorbent

Table. 9 Parameters of binary systems solutes isotherms for copper, zinc and nickel ions onto nanosorbent

Binary system				
Model	Parameter	$\text{Cu}^{+2}, \text{Zn}^{+2}$ system	$\text{Cu}^{+2}, \text{Ni}^{+2}$ system	$\text{Zn}^{+2}, \text{Ni}^{+2}$ system

		Cu ⁺²	Zn ⁺²	Cu ⁺²	Ni ⁺²	Zn ⁺²	Ni ⁺²
Extended Langmuir Equation(8)	q _m (mg/g)	17.157	3.841	8.939	2.537	8.922	2.2
	b (l/mg)	0.1	0.1	0.1	0.1	0.1	0.1
	R ²	0.752	-----	0.724	-----	0.555	
Redlich-Peterson Equation (9)	a,-	0.0083	9.107	0.008	144.54	0.0006	61.641
	β,-	1.882	0.2661	1.823	161.69	2.378	43.579
	R ²	0.822	0.944	0.785	-----	0.834	-----
Combination of Langmuir-Freundlich Equation (10)	q _m (mg/g)	1.4611	5.459	1.6034	4.9336	1.6257	2.7865
	b (l/mg)	2.0443	0.1	1.8949	0.1	2.157	0.1
	n	2.921	1.6664	2.962	1.6444	3.372	1.3481
	R ²	0.892	0.937	0.912	0.983	0.988	0.988

4.8 Ternary Component System

The adsorption isotherms for ternary component systems were correlated to which the best model was fitted in the binary component system. The parameters Table. 10 for the model were obtained from non-linear statistical fit of the equation to the experimental data.

The adsorption isotherms for ternary component system of Cu²⁺, Zn²⁺ and Ni²⁺ ions onto nanosorbent are shown in Fig.16

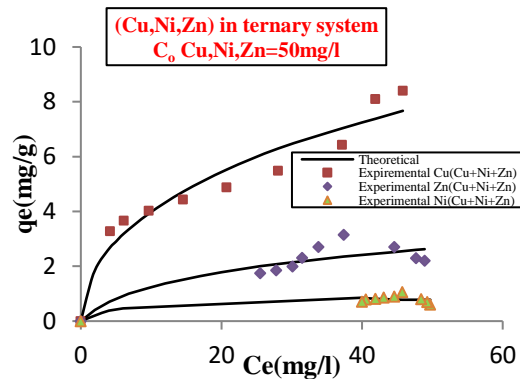


Fig.16 Adsorption isotherms of copper, zinc and nickel ions onto nanosorbent

Table.10 Parameters of ternary system isotherms for copper, zinc and nickel ions onto nanosorbent

Ternary system				
Model	Parameters	Cu ⁺² , Zn ⁺² , Ni ⁺² system		
		Cu ⁺²	Zn ⁺²	Ni ⁺²
Combination of Langmuir-Freundlich Equation (10)	q _m (mg/g)	1.306	0.483	0.727
	b (l/mg)	2.005	0.698	0.103
	n	2.130	1.308	1.152
	R ²	0.971	0.869	0.886

Fig.13 to 16 and Tables. 9 and 10 show the following:

- For each the binary and ternary systems the Combination of Langmuir- Freundlich model seems to give the best fitting for the experimental data at the highest value of R^2 . It can be seen from the Figures, Cu^{2+} always is adsorbed more favorable onto nanosorbent than Zn^{2+} and Ni^{2+} .
- The decrease of adsorption capacity in binary and ternary systems compared to the single metal systems was observed for all metals with exception of copper, reflects the existence of a competition between the metals studied for the binding sites present in nanoparticle wall. It seems that the total metal adsorption capacity onto the nanoparticle decreases when increasing the number of metals present. This fact supports the assumed competition between metals for the nano particle binding sites and tends to decrease the relative amount of each adsorbed element. These results agreed with the results obtained by [32].

Fig.s. 17 to 19 show that the metal removal efficiency of nanosorbent in single and mixed system was inhibited by the presence of the other heavy metals in the system. The removal efficiency of Cu^{2+} in the single system was 100% reduced to 96.1%,and 97.6%

respectively in the binary system with Zn^{2+} , and Ni^{2+} ions, while the removal efficiency of Cu^{2+} in the ternary system reduced to 91.62% with $[\text{Zn}^{2+} + \text{Ni}^{2+}]$. The removal efficiency of Zn^{2+} in the single system was 100% reduced to 64.8%,and 96% respectively in the binary system with Cu^{2+} , and Ni^{2+} ions, while the removal efficiency of Zn^{2+} in the ternary system reduced to 49% with $[\text{Cu}^{2+} + \text{Ni}^{2+}]$. The removal efficiency of Ni^{2+} in the single system was 82% reduced to 61%,and 58% respectively in the binary system with Zn^{2+} , and Cu^{2+} ions, while the removal efficiency of Ni^{2+} in the ternary system reduced to 20% with $[\text{Zn}^{2+} + \text{Cu}^{2+}]$.

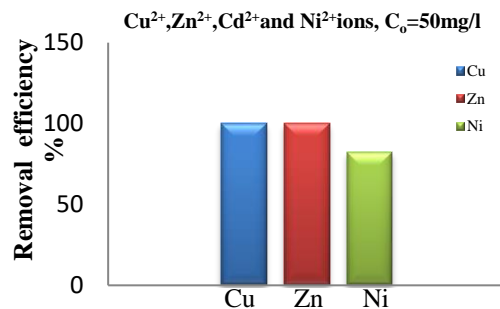


Fig. 17 Adsorption of copper, zinc and nickel ions, when used in single system

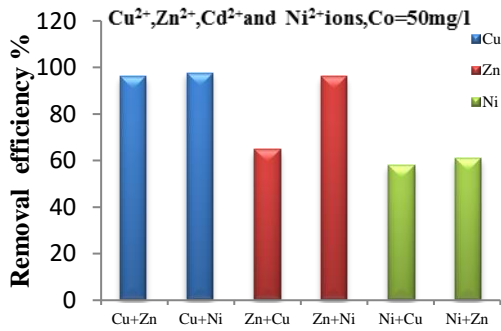


Fig. 18 Adsorption of copper, zinc and nickel ions, when used in binary system

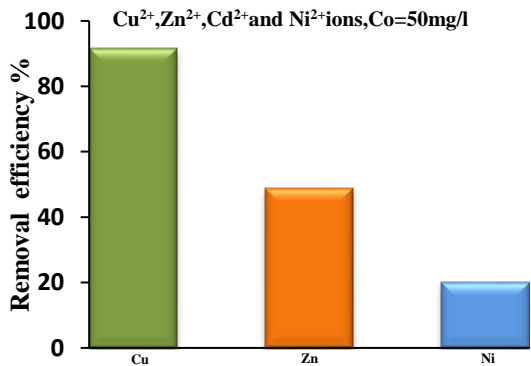


Fig. 19 Adsorption of copper, zinc and nickel ions, when used in ternary system

5. Conclusions

5.1 Single Component System

1. Optimum pH was 6 for Cu^{2+} , Zn^{2+} , and Ni^{2+} ions in adsorption process onto Fe_3O_4 nanoparticle (20-30 nm).
2. It can be concluded that 50 min contact time is sufficient to reach equilibrium condition for all heavy metals.
3. The equilibrium isotherm for each single component is of a favorable type and Freundlich isotherm gives

the best fit model for representing the experimental data.

4. In this system Cu^{2+} ions was the most favorable component rather than Zn^{2+} , and Ni^{2+} ions, due to its physiochemical characteristics, the lowest hydration Van der Waals radius and the electronegativities highest. Results for the three adsorbates in term of adsorption capacity were : $\text{Cu}^{2+} > \text{Zn}^{2+} > \text{Ni}^{2+}$.
5. It can be seen that the percentage removal efficiency was not altered greatly if the concentration increased from 10 to 50 mg/l, due to that the nanosorbent may contain enough sites for this concentration range, but when the concentrations increase to 100 and 150 mg/l the sites will not be enough to accumulate these concentrations so that the depletion in percentage removal was obvious.
6. Adsorption of Cu^{2+} , Zn^{2+} and Ni^{2+} ions was endothermic and physical in nature.

5.2 Binary and Ternary Component System

1. For each binary and ternary component systems, combination of Langmuir-Freundlich Isotherm gives the best fit for the experimental data. The behavior of the equilibrium isotherm is of favorable type.

2. For each system Cu^{2+} ions is still the most adsorbed component rather than Zn^{2+} , and Ni^{2+} ions.
3. Due to the competitive effect of Cu^{2+} , Zn^{2+} and Ni^{2+} ions with each other to occupy the available site(s) of the nanosorbent, Cu^{2+} ions offers the strongest component that is able to displace Zn^{2+} , and Ni^{2+} ions from their sites, while Ni^{2+} ions was the weakest adsorbed component.
4. Compared with their adsorption in the single component system the adsorption capacity of all three metals showed obvious decrease both in the binary and ternary system.
5. The percentage removal efficiency of each single component decreased in the binary and ternary system. This is due to the presence of more than one component will enhance the competitive struggling race for occupying a certain site.

6. References

1. Aksu, Z., Gönen, F., Demircan, Z., 2002, "*Biosorption of Chromium (VI) Ions by Mowital (R) B30H Resin immobilized Activated Sludge in a Packed Bed: Comparison with Granular Activated Carbon*", Process Biochem, 38,175–186.
2. Aldre, J., Morais, B., Shiva, P., Valderi D. L., Antonio, G. S., 2007, "*Biosorption of heavy metals in upflow sludge columns*", Bioresource Technology, 98 , 1418–1425.
3. APHA, 1995, "*Standard methods for the examination of water & wastewater*", 19th Edition, American Public Health Association , Washington, DC.
4. Bamgbose, J.T., Adewuyi, S., Bamgbose, O., Adetoye, A.A., 2010, "*Adsorption kinetics of cadmium and lead by chitosan* ", Afr. J. Biotechnol. 9 2560–2565.
5. Basha, S., and Murthy, Z., 2007, "*Kinetic and equilibrium models for biosorption of Cr(VI) on chemically modified seaweed cystoseir indica*", Adv. Environ. Res, 42(11), 1521-1529.
6. Bhaumik.M., Maity A., Srinivasu V.V., Onyango M.S. ,2012 ,"*Removal of hexavalent chromium from aqueous solution using polypyrrole-polyaniline nanofibers* ", Chemical Engineering Journal 181– 182 ,323– 333
7. César, V., Joan, I., Adriana, F., José L., 2010, "*Evaluating Binary Sorption of Phenol/Aniline from Aqueous Solutions onto Granular Activated Carbon and Hypercrosslinked Polymeric Resin (MN200)*", Water Air Soil Pollut, 210, 421–434.

8. Cheueh, I. Z., 2005, "*Ion Exchange Modeling of Silicotitanate Column for Chromium Removal from Argentine Waste*", Wisting house Savannah River Company, USA.
9. Chong, K., H., and Volesky, B., 1995, "*Metal biosorption equilibria in a ternary system*" *Biotechnology and Bioengineering* , 49(6), 629-638.
10. Colak, F., Atar, N., Olgun, A., 2009, "*Biosorption of acidic dyes from aqueous solution by Paenibacillus macerans: kinetic, thermodynamic and equilibrium studies*", *Chem. Eng. J.*, 150 (1) 122–130.
11. Fahmi, A. and Munther, K., 2003, "*Competitive Adsorption of Nickel and Cadmium on Sheep Manure Waste, Experimental and Prediction Studies*", *Separation Science and Technology*, 38 (2), pp 483-497.
12. Feng, Y., Gong, J.-L., Zeng, G.-M., Niu, Q.-Y., Zhang, H.-Y., Niu, C.-G., Deng J.-H., Yan ,M., 2010 , "*Adsorption of Cd (II) and Zn (II) from aqueous solutions using magnetic hydroxyapatite nanoparticles as adsorbents*", *Chem. Eng. J.* 162 487–494.
13. Gray, N.F., 2005, "*Water technology; an introduction for environmental scientist's engineers*", Second edition, Elsevier Butterworth-Heinemann.
14. Grossl, P.R., Sparks, D.L., Ainsworth, C.C., 1994, "*Rapid kinetics of Cu(II) adsorption-desorption on goethite*", *Environ. Sci. Technol.* 28 1422–1429.
15. Gupta ,V.K. and ,Nayak, A. ,2012 , "*Cadmium removal and recovery from aqueous solutions by novel adsorbents prepared from orange peel and Fe₂O₃ nanoparticles*" *Department of Chemistry, Indian Institute of Technology Roorkee, Roorkee 247667, India Chemical Engineering Journal* 180 81– 90.
16. Gupta V.K., Agarwal, S., Saleh, T.A., 2011, "*Synthesis and characterization of alumina coated carbon nanotubes and their application for lead removal*", *J. Hazard. Mater.* 185 17–23.
17. Hasany, S.M., Saeed, M.M., and Ahmed, M., 2002, "*Sorption and thermodynamic behavior of Zn(II)-thiocyanate complexes onto polyurethane foam from acidic solutions*", *J. Radioanal. Nucl. Chem.*, 252(3), 477–484.
18. Hawari, H A., and Mulligan N. C, 2006, "*Biosorption of lead(II), cadmium(II), copper(II) and nickel(II) by anaerobic granular biomass*", *Bioresource technology*, 97, 692-700.
19. Hizal J., and Apak, R., 2006, "*Modeling of cadmium (II) adsorption on kaolinite-based clays in the absence and presence*

- of humic acid*", Appl. Clay Sci. 32 232–244.
20. Hu J, Chen, G.H., Lo I.M.C., 2005, "*Removal and recovery of Cr (VI) from wastewater by maghemite nanoparticles*", Water Res; 39(18) : 4528–36.
 21. Huang, X., Gao, N.Y., Zhang, Q.L., 2007, "*Thermodynamics and kinetics of cadmium adsorption onto oxidized granular activated carbon*", J. Environ. Sci. 19 1287–1292.
 22. Jianlong, W., and Can, C., 2009, "*Biosorbents for heavy metals removal and their future*", Biotechnology Advances, 27, 195–226.
 23. Khan, M. H., Keshtkar, A. R., Meysami B., Zarea, M. F., Jalali, R., 2006, "*Biosorption of uranium from aqueous solutions by nonliving biomass of marine algae Cystoseira indica*", Electronic Journal of Biotechnology, 9 (2), 100-106.
 24. Kratochvil, D., and Volesky, B., 1998, "*Advances in Biosorption of Heavy Metals*", Trend in Biotechnology, 16, 291-300.
 25. Lawrence, K. Wang, J. T., Stephen, T.T., Yung-Tse H., 2010, "*Handbook of environmental engineering, environmental bioengineering*", Springer New York Dordrecht Heidelberg London.
 26. Lin, C-C, and Lai, Y-T., 2006, "*Adsorption and recovery of lead(II) from aqueous solutions by immobilized Pseudomonas aeruginosa R08 beads*", J Hazard Mater, 137(105), 99–105.
 27. Liu, J.F., Zhao, Z.S., Jiang, G.B., 2008, "*Coating Fe₃O₄ magnetic nanoparticles with humic acid for high efficient removal of heavy metals in water*", Environ. Sci. Technol. 42 6949–6954.
 28. Manhan, S. T., 2005, "*Controlling Heavy Metal in Water by Adsorption*", Bio. Che. J., 60(7), pp 801-803.
 29. Marcus, Y. and Kertes, A.S, 1969, "*Ion exchange and solvent extraction of metal complexes*", Johan Wiley and Sons, London, UK.
 30. Mashitah, M.D., Yus Azila, Y., Bhatia, S., 2008, "*Biosorption of cadmium (II) ions by immobilized cells of Pycnoporus sanguineus from aqueous solution*", Bioresour. Technol, 99, 4742–4748.
 31. Maurya, N.S., Mitta, A.K., Cornel, P., Rother, E., 2006, "*Biosorption of dyes using dead macro fungi: effect of dye structure, ionic strength and pH*", Biores Technol, 97(21), 512–521.
 32. Nassar, N.N. ,(2010) , "*Rapid removal and recovery of Pb(II) from wastewater by magnetic nanoadsorbents*", Department of

- Chemical and Petroleum Engineering, University of Calgary, Calgary, Alberta, Canada
- ,Journal of Hazardous Materials 184 538–546
- 33.Öztürk, A., Artan, T., Ayar, A., 2004, "*Biosorption of nickel(II) and copper(II) ions from aqueous solution by Streptomyces coelicolor*", A3(2), Colloids and Surfaces B: Biointerfaces, 34(2), 105-111.
- 34.Padmavathy, V., 2008, "*Biosorption of nickel(II) ions by baker's yeast: Kinetic, thermodynamic and desorption studies*", Bioresource Technology 99, 3100–3109.
- 35.Padmesh, T., Vijayaraghavan, K., Sekaran, G., Velan, M., 2006, "*Application of Azolla rongpong on biosorption of acid red 88, acid green 3, acid orange 7 and acid blue 15 from synthetic solutions*", Chemical Engineering Journal, 122, 55–63.
- 36.Panda ,G.C., Das, S.K., Guha ,A.K., 2008 , "*Biosorption of cadmium and nickel by functionalized husk of Lathyrus sativus*", Colloids Surf. B: Biointerfaces 62 173–179.
- 37.Panuccio ,M.R., Sorgonà, A., Rizzo, M., Cacco, G., 2009 , "*Cadmium adsorption on vermiculite zeolite and pumice: batch experimental studies*" ,J.Environ .Manage. 90 364–374.
- 38.Rao, C. S., 1994, "*Environmental Pollution Control Engineering*", Wiley Estern, India.
39. Ridha, M.J., 2011, "*Competitive Biosorption of Heavy Metals Using Expanded Granular Sludge Bed Reactor*", Ph.D. Thesis, University of Baghdad, College of Engineering.
- 40.Sahmoune, M., Louhab, K., Boukhiar, A., 2009, "*Biosorption of Cr(iii) from aqueous solutions using bacterium biomass streptomyces rimosus*", Int. J. Environ. Res., 3(2), 229-238.
- 41.Saleem, M., Chakrabarti, M.H., Irfan, M.F., Hajimolana, S.A., Hussain, M.A., 2011," *Electrokinetic remediation of nickel from low permeability soil*", Int. J. Electrochem. Sci., 96, 4264-4275.
- 42.Sevgi ,K., 2009 , "*Adsorption of Cd (II), Cr (III) and Mn (II) on natural sepiolite*", Desalination 244 24–30.
- 43.Shen, Y.F., Tang, J., Nie, Z.H., Wang, Y.D., Ren Y., Zuo, L., 2009, "*Preparation and application of magnetic Fe₃O₄ nanoparticles for wastewater purification*", Sep. Sci. Technol.68 312–319.
- 44.Shin, E.W., Karthikeyan, K.G., Tshabalala, M.A., 2007, "*Adsorption mechanism of cadmium on juniper bark and wood*", Bioresour. Technol. 98 588–594.

45. Sips, R., 1984, "On the structure of a catalyst surface", J. Chem. Phys., 16, 490-495.
46. Srivastava V., Weng, C.H., Singh, V.K., Sharma, Y.C., 2011, "Adsorption of nickel ions from aqueous solutions by nano alumina: kinetic, mass transfer, and equilibrium studies", J. Chem. Eng. Data 56 1414–1422.
47. Sulaymon, A. H., and Ahmed, K. W., 2008, "Competitive adsorption of furfural and phenolic compounds onto activated carbon in fixed bed column", Environ. Sci. Technol. 42 (2), 392–397.
48. Sulaymon, H. A., Abidb, A. B., Al-Najar, A. J., 2009, "Removal of lead copper chromium and cobalt ions onto granular activated carbon in batch and fixed-bed adsorbers", Chemical Engineering Journal. 155(3), 647-653
49. Taghi, g., Khosravi, M., Rakhshae, R., 2005, "Biosorption of Pb, Cd, Cu and Zn from the wastewater by treated *Azolla filiculoides* with $H_2O_2/MgCl_2$ ", International Journal of Environmental Science & Technology, 1(4), 265-271.
50. Vijayaraghavan, K., Sung, W. W., Yeoung-S, Y., 2008, "Single- and dual-component biosorption of reactive black 5 and reactive orange 16 onto polysulfone-immobilized esterified *Corynebacterium glutamicum*", Ind. Eng. Chem. Res. 47, 3179-3185.
51. Vijayaraghavan, K., Yun, Y.S., 2008, "Bacterial biosorbents and biosorption", Biotechnology Advances, 26, 266–291.
52. Wang, J., and Chen, C., 2009, "Biosorbents for heavy metals removal and their future", Biotechnology Advances, 27, 195–226.
53. Xu, P., Zeng, M., G., Huang, L., D., Feng, L., C., Shuang, H., S., Zhao, H., M., Lai, C., Wei, Z., Huang, C., Xie, X., G., Liu, F., Z., 2012, "Use of iron oxide nanomaterials in wastewater treatment: A review" Science of the Total Environment 424 1–10
54. Zubeyde, B., Ercan, C., Mehmet, D., 2009, "Equilibrium and thermodynamic studies on biosorption of Pb(II) onto *Candida albicans* biomass", Hazardous Materials 161, 62–67.

الازالة التنافسية لأيونات النحاس والزنك والنيكل بواسطة مادة نانوية (اوكسيد الحديد)

أ.م.د. شهلاء اسماعيل ابراهيم
 قسم هندسة البيئة
 حسنين سعد عبد الزهرة
 كلية الهندسة / جامعة بغداد
 بغداد العراق
الخلاصة:-

الدراسة الحالية تهدف الى تقييم عملية الامتزاز للمعادن الثقيلة (النحاس، النيكل والزنك) من المياه المصنعة مختبريا بواسطة مادة نانوية. وتم شراء مادة نانوية مازة وهي اوكسيد الحديد (Fe_3O_4) من الولايات المتحدة الامريكية. تمت دراسة تغيير بعض العوامل المختبرية على عملية الامتزاز مثل الدالة الحامضية، التركيز الاولي للمعادن، والحرارة. من النتائج المختبرية ان سعة الامتزاز هي 9.8,6.07,11.5 ملغ/غم لأيونات النحاس والنيكل والزنك على التوالي باستخدام مادة النانو. وجد ان أفضل نسب الازالة لمادة النانو تحصل عند قيمة الحامضية 6 لجميع الايونات وان وقت التماس الامثل هو 50 دقيقة. تم القيام بسلسلة من تجارب الدفعات (batch experiment) للملوثات بصورة منفردة وثنائية وثلاثية لغرض الحصول على مخططات الامتزاز لكل ملوث. وقد وجد أن موديل (Freundlich) ، أفضل موديل رياضي يمثل النتائج العملية بالنسبة للمنفردة. اما بالنسبة الى التجارب الثنائية والثلاثية ، وجد ان موديل (Combination of Langmuir- Freundlich) افضل موديل رياضي يمثل النتائج العملية. وقد تميزت ايونات النحاس بأعلى قدرة وملائمة على الامتزاز بواسطة مادة النانو بينما ايونات النيكل اقل قدرة من بقية الايونات. كما وجد ان طبيعية الامتزاز للمعادن الثقيلة هو ماص للحرارة من خلال التجارب الحرارية (thermodynamic study) وذو طبيعة فيزيائية.